J. Phys. Chem. A **2009,** *113,* 12163–12170 **12163**

Reactions of Group 14 Metal Atoms with Acetylene: A Matrix Isolation Infrared Spectroscopic and Theoretical Study

Yun-Lei Teng and Qiang Xu*

National Institute of Advanced Industrial Science and Technology (AIST), Ikeda, Osaka 563-8577, and Graduate School of Engineering, Kobe University, Nada Ku, Kobe, Hyogo 657-8501, Japan

Received: March 5, 2009; Revised Manuscript Received: September 21, 2009

Laser-ablated group 14 metal atoms have been codeposited at 4 K with acetylene in excess argon. Products, Ge(C_2H_2), HGeCCH, Sn(C_2H_2), Sn_2CCH_2, HSnCCH, and HPbCCH, have been formed in the present experiments and characterized using infrared spectroscopy on the basis of the results of the isotopic shifts, mixed isotopic splitting patterns, stepwise annealing, the change of reagent concentration and laser energy, and the comparison with theoretical predictions. Density functional theory calculations have been performed on these molecules. The agreement between the experimental and the calculated vibrational frequencies, relative absorption intensities, and isotopic shifts supports the identification of these molecules from the matrix infrared spectra. Plausible reaction mechanisms have been proposed to account for the formation of these molecules.

Introduction

Considerable attention has been paid to the interactions of metal atoms with acetylene due to the industrial importance of hydrocarbon hydrogenation and dehydrogenation processes.[1–3] The interactions of metal atoms with acetylene have been investigated using the matrix isolation technique, and four bonding models, side-on M-η^2-(C_2H_2) (Cu, Ag, Au, Cr, Ni, Al, Pt, Pd, Li, U, Th, La, Ti, Zr, Hf), vinyl form M-C_2H_2 (Al, Au), inserted HMCCH (Be, B, Cr, Pt, Al, Fe, Cr, La, Ti, Zr, Hf), and vinylidene M=C=CH_2 (Ni, Au, Pt, Na, La) have been identified and characterized by infrared and electron spin resonance spectroscopies.[4–17] In addition, different kinds of products, M(C_2H_2)$_2$ (Pd, U, Th), MCCH (Mg, U, Th), and Pd_2(C_2H_2), have also been identified and characterized through the matrix isolation technique.[11,17,18] The interactions of metal with acetylene have also been extensively investigated by quantum chemical computations.[18–22] The reactions of group 14 metal atoms with C_2H_2 have not been investigated using both the experimental and the theoretical methods. The germanium−acetylene and tin−acetylene polymers have been prepared and characterized, and the adsorption of acetylene on the Ge(001) surface have been investigated using the first-principles pseudopotential technique.[22,23] However, as far as we know, the reactions of group 14 metal atoms with acetylene have not been studied using the matrix isolation techniques.

Recent studies have shown that, with the aid of isotopic substitution techniques, matrix isolation infrared spectroscopy combined with quantum chemical calculations is very powerful for investigating structure and bonding of novel species.[14–17,24,25] To understand the interaction of acetylene and group 14 metal atoms, the reactions of laser-ablated group 14 metal atoms with acetylene in a solid-argon matrix have been performed. IR spectroscopy and theoretical calculations provide evidence for the formation of products, Ge(C_2H_2), HGeCCH, Sn(C_2H_2), Sn_2CCH_2, HSnCCH, and HPbCCH.

Experimental and Theoretical Methods

The experiment for laser ablation and matrix-isolation infrared spectroscopy is similar to those previously reported.[25] Briefly, the Nd:YAG laser fundamental (1064 nm, 10 Hz repetition rate with 10 ns pulse width) was focused on the rotating group 14 metal targets. The laser-ablated group 14 metal atoms were codeposited with C_2H_2 (99.96%, Cambridge Isotopic Laboratories) in excess argon onto a CsI window cooled normally to 4 K by means of a closed-cycle helium refrigerator. Typically, a 3−10 mJ/pulse laser power was used. The isotopic $^{13}C_2H_2$ and C_2D_2 (99%, Cambridge Isotopic Laboratories) were used to prepare the C_2H_2/Ar mixtures. In general, matrix samples were deposited for 30−60 min with a typical rate of 2−4 mmol per hour. After sample deposition, IR spectra were recorded on a Bruker IFS 66v/s spectrometer at 0.5 cm^{-1} resolution using a liquid nitrogen cooled HgCdTe (MCT) detector for the spectral range of 5000−600 cm^{-1}. Samples were annealed at different temperatures and subjected to broadband irradiation ($\lambda > 250$ nm) using a high-pressure mercury arc lamp (Ushio, 100 W).

Quantum chemical calculations were performed to predict the structures and vibrational frequencies of the observed reaction products using the Gaussian 03 program.[26] The B3LYP and B3PW91 density functional methods were utilized.[27] The 6-311++G(d, p) basis set was used for Ge, H, and C atoms, and LANL2DZ was used for Sn and Pb atoms.[28,29] Geometries were fully optimized and vibrational frequencies were calculated with analytical second derivatives. Transition-state optimizations were done with the synchronous transit-guided quasi-Newton (STQN) method.

Results and Discussion

Experiments have been done with C_2H_2 concentrations ranging from 0.05% to 0.5% in excess argon. Typical infrared spectra for the reactions of laser-ablated group 14 metal atoms with C_2H_2 in excess argon in the selected regions are illustrated in Figures 1−9, and the absorption bands are listed in Table 1. The stepwise annealing and irradiation behaviors of these product absorptions are also shown in the figures and will be discussed below.

---

* Author to whom correspondence should be addressed. E-mail: q.xu@aist.go.jp.

10.1021/jp902041f CCC: $40.75

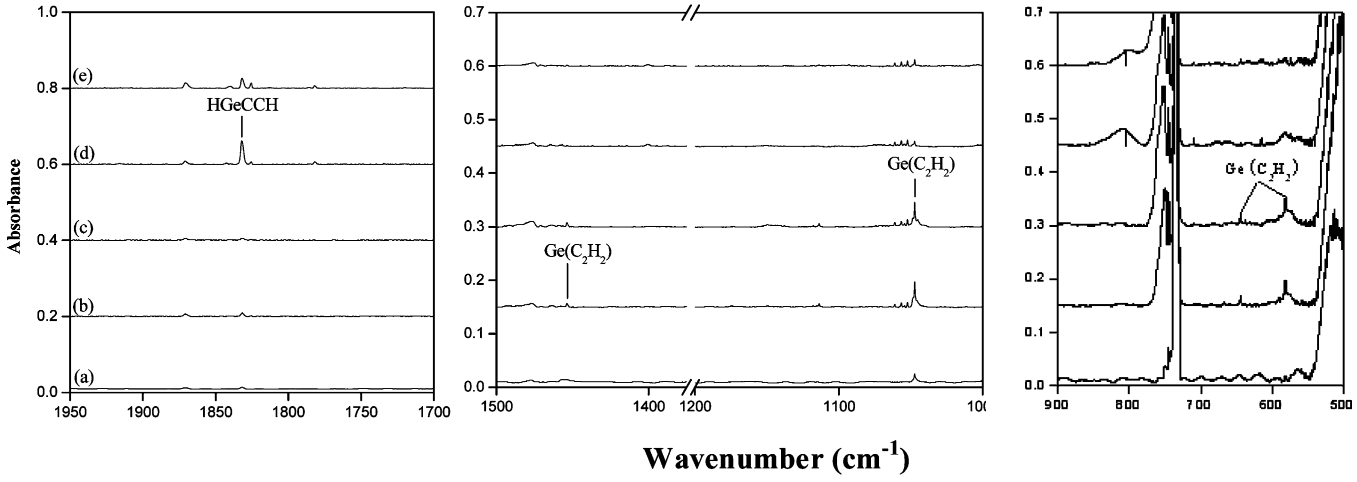

Figure 1. Infrared spectra in the 1950−1700, 1500−1000, and 900–500 cm^{-1} regions from codeposition of laser-ablated Ge atoms with 0.4% C_2H_2 in argon: (a) 60 min sample deposition at 4 K, (b) after annealing to 25 K, (c) after annealing to 30 K, (d) after 15 min of broadband irradiation, and (e) after annealing to 35 K.

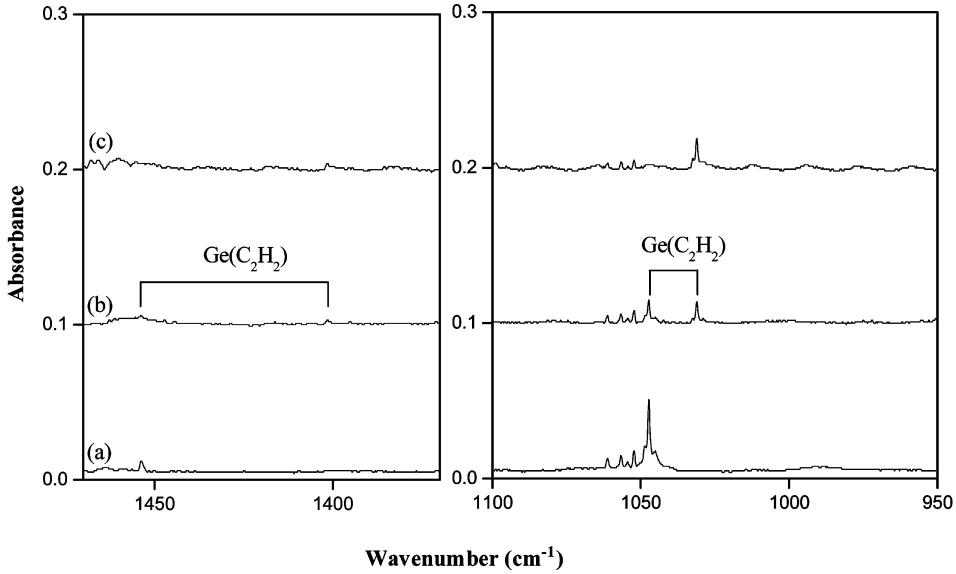

Figure 2. Infrared spectra in the 1470−1370 and 1100−950 cm^{-1} regions from codeposition of laser-ablated Ge atoms with C_2H_2 in argon: (a) 0.4% $^{12}C_2H_2$, (b) 0.3% $^{12}C_2H_2$ + 0.3% $^{13}C_2H_2$, and (c) 0.4% $^{13}C_2H_2$.

Quantum chemical calculations have been carried out for the possible isomers and electronic states of the potential product molecules. Figure 10 shows the optimized structures and electronic ground states. Tables 2−7 report the calculated IR frequencies and isotopic frequencies of the reaction products. The results of the B3PW91 calculation are consistent with those of the B3LYP calculation.

Ge(C_2H_2). The absorptions at 1453.1, 1045.9, 644.5, and 582.6 cm^{-1} can be grouped together to one species, on the basis of the growth/decay characteristics as a function of changes of experimental conditions. The four bands appear on sample deposition, visibly increase on sample annealing to 25 K, further increase on annealing to 30 K, and disappear after broadband irradiation (Table 1 and Figure 1). The 1453.1 cm^{-1} band shifts to 1402.0 cm^{-1} with $^{13}C_2H_2$, exhibiting isotopic frequency ratio of 1.0364 ($^{12}C_2H_2$/$^{13}C_2H_2$) indicates that the 1453.1 cm^{-1} band should be assigned to a C−C stretching vibration.[14] As shown in Figure 2, the mixed $^{12}C_2H_2$ + $^{13}C_2H_2$ isotopic spectra only provide the sum of pure isotopic bands, which indicates that it is possible that only one C_2H_2 subunit is involved in this mode. Therefore, the 1453.1 cm^{-1} band is assigned to the C−C stretching vibration of the Ge(C_2H_2) molecule. The C−C

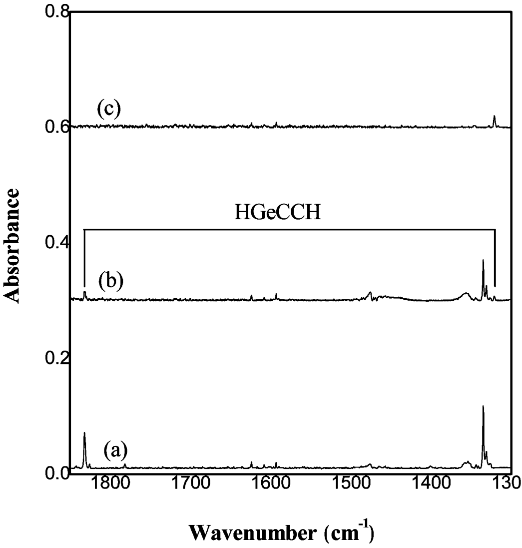

Figure 3. Infrared spectra in the 1850−1300 cm^{-1} region from codeposition of laser-ablated Ge atoms with C_2H_2 in argon: (a) 0.4% $^{12}C_2H_2$, (b) 0.2% $^{12}C_2H_2$ + 0.2% C_2D_2, and (c) 0.4% C_2D_2.

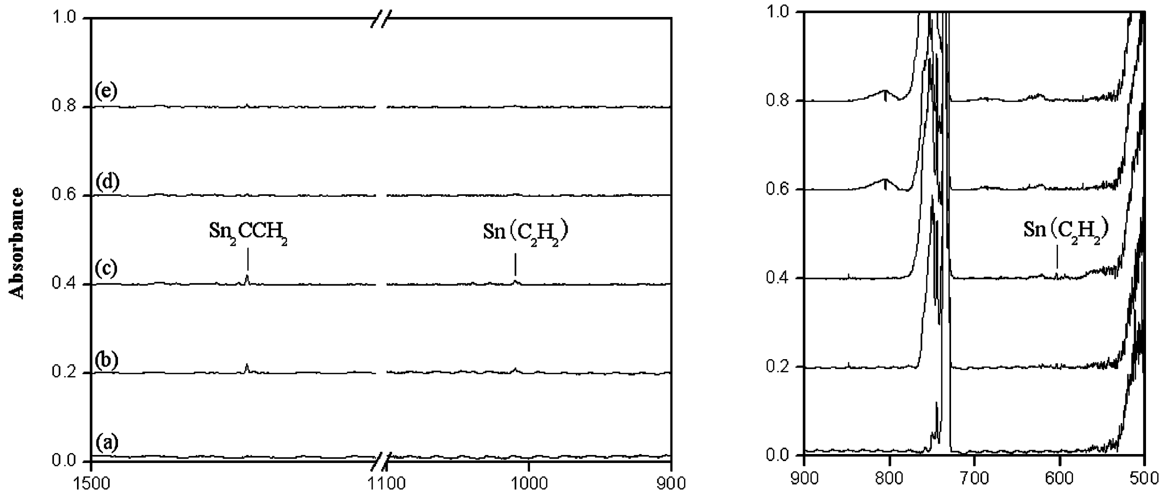

Figure 4. Infrared spectra in the 1500−900 and 900−500 cm^{-1} regions from codeposition of laser-ablated Sn atoms with 0.4% C_2H_2 in argon: (a) 60 min sample deposition at 4 K, (b) after annealing to 25 K, (c) after annealing to 30 K, (d) after 15 min of broadband irradiation, and (e) after annealing to 35 K.

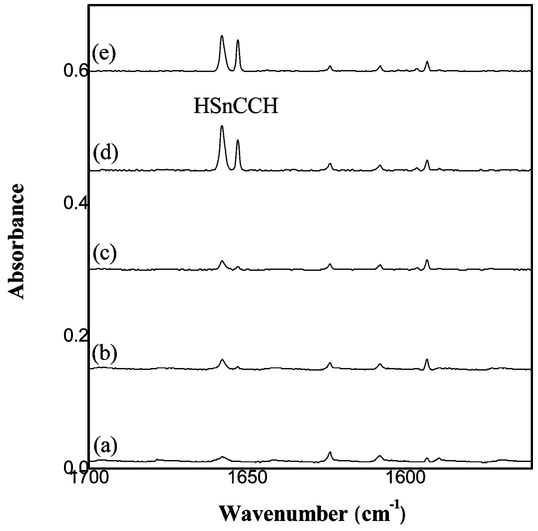

Figure 5. Infrared spectra in the 1700−1560 cm^{-1} region from codeposition of laser-ablated Sn atoms with 0.4% C_2H_2 in argon: (a) 60 min sample deposition at 4 K, (b) after annealing to 25 K, (c) after annealing to 30 K, (d) after 15 min of broadband irradiation, and (e) after annealing to 35 K.

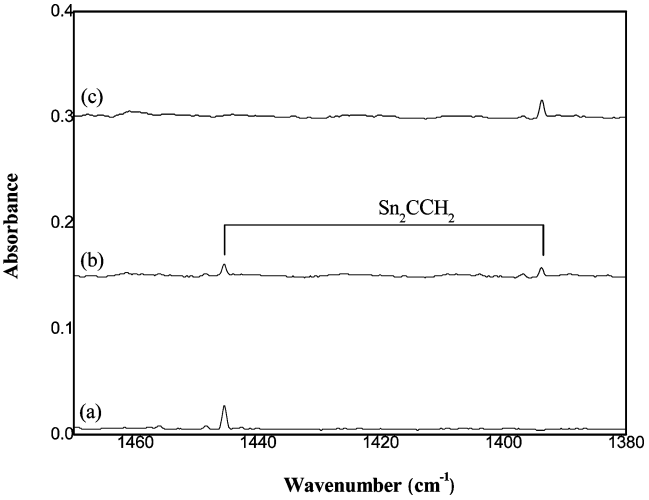

Figure 6. Infrared spectra in the 1470−1380 cm^{-1} region from codeposition of laser-ablated Sn atoms with C_2H_2 in argon: (a) 0.4% $^{12}C_2H_2$, (b) 0.2% $^{12}C_2H_2$ + 0.2% $^{13}C_2H_2$, and (c) 0.4% $^{13}C_2H_2$.

stretching frequency is significantly lower than that of previous reported transition metal−acetylene π complexes $Ni(C_2H_2)$ (1647 cm^{-1})[7] and $Cu(C_2H_2)$ (1870 cm^{-1})[4] and is close to the value of metallacyclopropene, $H_2Ti(C_2H_2)$ (1465 cm^{-1})[9b] and $Cr(C_2H_2)$ (1476 cm^{-1}),[14] in solid argon, indicating that $Ge(C_2H_2)$ is not a π complex but should be considered as a metallacyclopropene. The C−C stretching vibrational frequency of $Ge(C_2H_2)$ at 1453.1 cm^{-1} is about 519 cm^{-1} red-shifted from the C−C stretching frequency of acetylene and is about 175 cm^{-1} lower than the C−C stretching frequency of ethylene.[30] The 1045.9 cm^{-1} band tracks with the 1453.1 cm^{-1} band, suggesting a different mode of the same molecule. The 1045.9 cm^{-1} band shifts to 1030.2 cm^{-1} with $^{13}C_2H_2$ and is due to the CCH deformation mode. For this band, the mixed $^{12}C_2H_2$ + $^{13}C_2H_2$ isotopic spectrum only provides the sum of pure isotopic bands, which also indicates that it is possible that only one C_2H_2 subunit is involved in this mode (Figure 2). The 644.5 and 582.6 cm^{-1} bands, which shift to 642.6 and 567.9 cm^{-1} with $^{13}C_2H_2$, respectively, are due to the C_2H_2 tilt and Ge−C stretching modes. However, the C_2D_2 counterparts of the 1453.1, 1045.9, 644.5, and 582.6 cm^{-1} bands are not observed. Observations using the C_2HD monodeuterated acetylene precursor may be very useful to prove the identification. In addition, experiments with different C_2H_2 concentration and laser energy have been performed, through which we can conclude that there may be only one C_2H_2 subunit and one Ge atom in the product.

The assignment is strongly supported by DFT calculations. As shown in Figure 10 and Table 2, the $Ge(C_2H_2)$ molecule is predicted to have an $^1A_1$ ground state with C_{2v} symmetry (Figure 10) and is the most stable structural isomer of Ge−C_2H_2. The C−C stretching, CCH deformation, C_2H_2 tilt, and Ge−C stretching modes are calculated at 1500.8, 1072.4, 665.9, and 574.8 cm^{-1} (Table 2), which are in good agreement with the experimental observations (1453.1, 1045.9, 644.5, and 582.6 cm^{-1}). The isotopic frequency ratios calculated for the C−C stretching, CCH deformation, C_2H_2 tilt, and Ge−C stretching modes ($^{12}C_2H_2$/$^{13}C_2H_2$, 1.0379, 1.0158, 1.0055, and 1.0264) are also consistent with the experimental observations ($^{12}C_2H_2$/$^{13}C_2H_2$, 1.0364, 1.0152, 1.0030, and 1.0259). These agreements between the experimental and the calculated vibrational frequencies, relative absorption intensities, and isotopic shifts confirm the identification of the $Ge(C_2H_2)$ molecule from the matrix IR spectra.

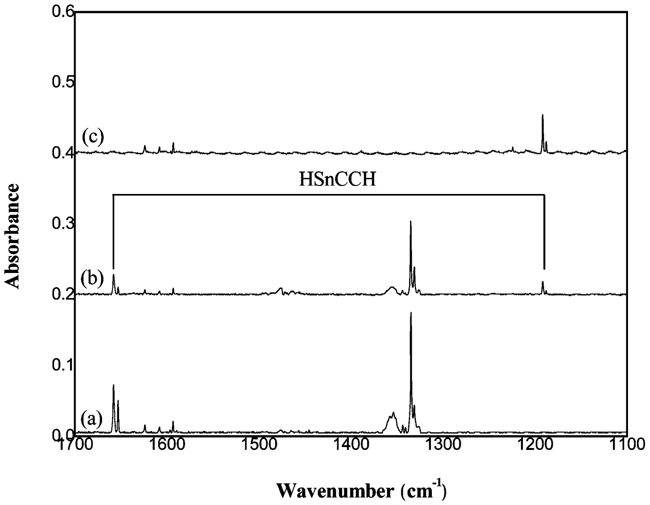

Figure 7. Infrared spectra in the 1700−1100 cm^{-1} region from codeposition of laser-ablated Sn atoms with C_2H_2 in argon: (a) 0.4% $^{12}C_2H_2$, (b) 0.2% $^{12}C_2H_2$ + 0.2% C_2D_2, and (c) 0.4% $^{13}C_2D_2$.

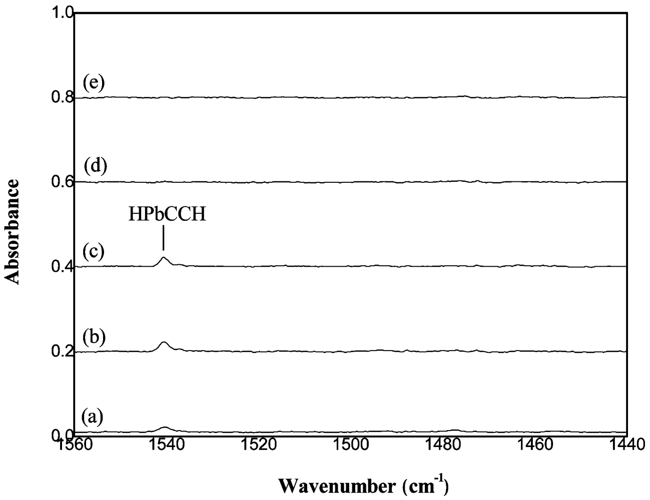

Figure 8. Infrared spectra in the 1560−1440 cm^{-1} region from codeposition of laser-ablated Pb atoms with 0.4% C_2H_2 in argon: (a) 60 min sample deposition at 4 K, (b) after annealing to 25 K, (c) after annealing to 30 K, (d) after 15 min of broadband irradiation, and (e) after annealing to 35 K.

HGeCCH. A new band at 1831.3 cm^{-1} (Table 1 and Figure 1) appears after broadband irradiation, decreases on further annealing to 35 K. The band is assigned to the HGeCCH molecule on the basis of isotopic substitution and DFT calculations. The 1831.3 cm^{-1} band shows no carbon-13 shift but shifts to 1319.9 cm^{-1} with $^{12}C_2D_2$, exhibiting isotopic frequency ratio of 1.3875 ($^{12}C_2H_2$/$^{12}C_2D_2$). The band position and the isotopic $^{12}C_2H_2$/$^{12}C_2D_2$ ratio are close to the values of the Ge−H stretching vibration of various previously characterized Ge hydrides in excess argon,[31] implying that the 1831.3 cm^{-1} band is due to a Ge−H stretching vibration. The mixed $^{12}C_2H_2$ + C_2D_2 isotopic spectra only provide the sum of pure isotopic bands, which indicates that only one Ge−H subunit is involved in this mode (Figure 3). Therefore, the 1831.3 cm^{-1} band is assigned to the Ge−H stretching vibration of the HGeCCH molecule.

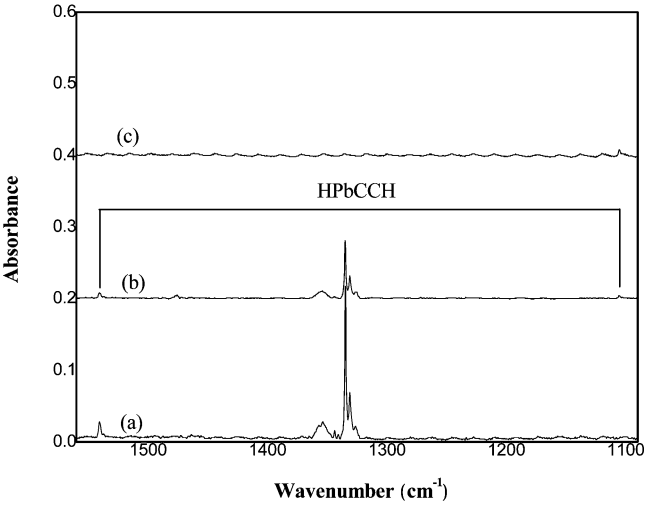

Figure 9. Infrared spectra in the 1560−1100 cm^{-1} region from codeposition of laser-ablated Pb atoms with C_2H_2 in argon: (a) 0.4% $^{12}C_2H_2$, (b) 0.2% $^{12}C_2H_2$ + 0.2% C_2D_2, and (c) 0.4% $^{13}C_2D_2$.

TABLE 1: Infrared Absorptions (cm^{-1}) from Co-Deposition of Laser-Ablated Group 14 Metal Atoms with Acetylene in Excess Argon

$^{12}C_2H_2$	$^{13}C_2H_2$	$^{12}C_2D_2$	assignment
1453.1	1402.0		$Ge(C_2H_2)$, C−C stretching
1045.9	1030.2		$Ge(C_2H_2)$, -plane CCH deformation
644.5	642.6		$Ge(C_2H_2)$, C_2H_2 tilt
582.6	567.9		$Ge(C_2H_2)$, Ge−C streching
1831.3		1319.9	HGeCCH, Ge−H stretching
1445.4	1393.8		Sn_2CCH_2, C−C stretching
1008.4	986.4		$Sn(C_2H_2)$, in-plane CCH deformation
604.1	603.7		$Sn(C_2H_2)$, C_2H_2 tilt
1657.9		1187.2	HSnCCH, Sn−H stretching
1541.3		1105.6	HPbCCH, Pb−H stretching

The present calculations lend support for the assignment of HGeCCH. Our calculations predict that HGeCCH has an $^1A'$ ground state with C_s symmetry (Figure 10). The Ge−H stretching vibrational frequency is calculated at 1890.8 cm^{-1} (Table 3), which is in agreement with the experimental observation (1831.3 cm^{-1}). The calculated $^{12}C_2H_2$/$^{12}C_2D_2$ isotopic frequency ratio (1.3996) of Ge−H stretching mode is also consistent with the experimental observation. The C−C stretching and CCH bending modes are not observed in the present experiment, probably because of the isomerization to other molecules under the broadband irradiation, which results in weak intensity. These agreements between the experimental and the calculated vibrational frequencies, relative absorption intensities, and isotopic shifts confirm the identification of the HGeCCH molecule from the matrix IR spectra.

$Sn(C_2H_2)$. A new absorption at 1008.4 cm^{-1} appears on sample annealing to 25 K, further increases on annealing to 30 K, and disappears after broadband irradiation (Table 1 and Figure 4). The 1008.4 cm^{-1} band shifts to 986.4 cm^{-1} with $^{13}C_2H_2$, exhibiting isotopic frequency ratios of 1.0223 ($^{12}C_2H_2$/$^{13}C_2H_2$). The band position and the isotopic frequency ratio indicate that the 1008.4 cm^{-1} band should be assigned to a CCH deforming vibration.[14] The mixed $^{12}C_2H_2$ + $^{13}C_2H_2$ isotopic spectrum only provides the sum of pure isotopic bands, which indicates that only one C_2H_2 subunit is involved in this mode. The 604.1 cm^{-1} band tracks with the 1008.4 cm^{-1} band, suggesting a different mode of the same molecule. The 604.1 cm^{-1} band that shifts to 603.7 cm^{-1} with $^{13}C_2H_2$ is due to the C_2H_2 tilt mode. Therefore, the 1008.4 and 604.1 cm^{-1} bands are assigned to the CCH deforming and C_2H_2 tilt vibrations of the $Sn(C_2H_2)$ molecule.

The assignment is supported by DFT calculations. As shown in Figure 10 and Table 4, the $Sn(C_2H_2)$ molecule is predicted to have an $^1A_1$ ground state with C_{2v} symmetry (Figure 10) and is the most stable structural isomer of $Sn-C_2H_2$. The C−C

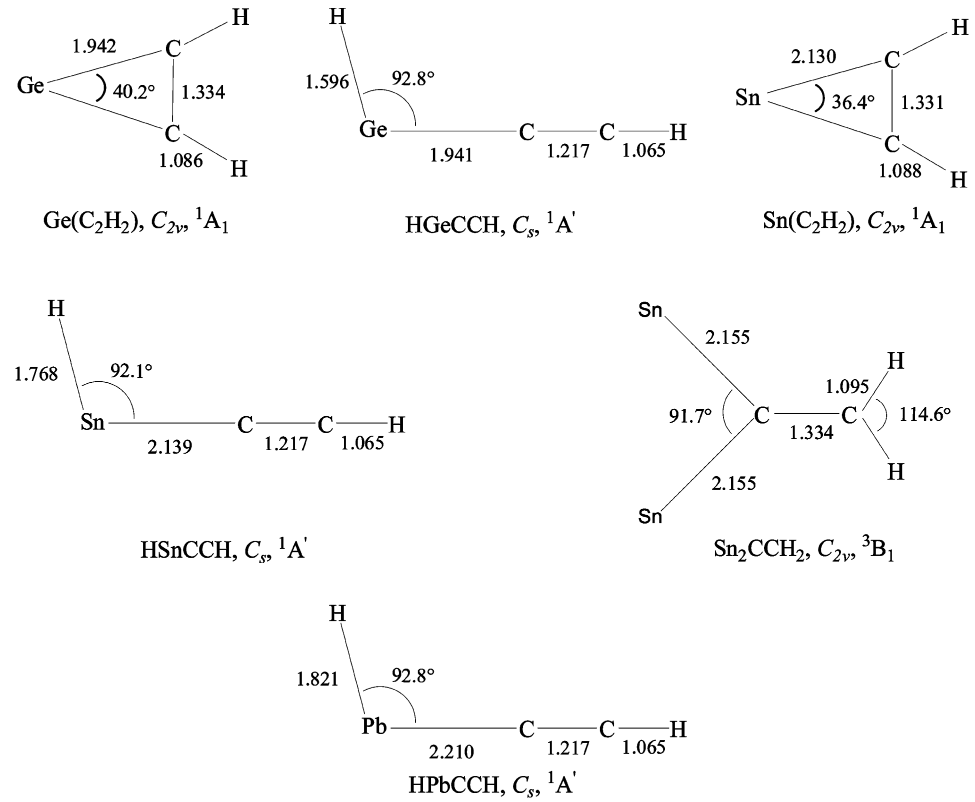

Ge(C_2H_2), C_{2v}, $^1A_1$

HGeCCH, C_s, $^1A'$

Sn(C_2H_2), C_{2v}, $^1A_1$

HSnCCH, C_s, $^1A'$

Sn_2CCH_2, C_{2v}, $^3B_1$

HPbCCH, C_s, $^1A'$

Figure 10. Optimized structures (bond length in angstrom, bond angle in degree) of the possible products calculated at the B3LYP level.

TABLE 2: Calculated (B3LYP and B3PW91/6-311++G(d,p)) Vibrational Frequencies and Intensities of Ge(C_2H_2) ($^1A_1$)[a]

Ge($^{12}C_2H_2$)	Ge($^{13}C_2H_2$)	Ge($^{12}C_2D_2$)	mode
		B3LYP	
3164.7 (10)	3152.0 (12)	2382.1 (1)	symm C−H stretching
3136.7 (10)	3127.4 (11)	2312.2 (3)	antisymm C−H stretching
1500.8 (7)	1446.0 (7)	1440.3 (6)	C−C stretching
1072.4 (67)	1055.7 (70)	909.1 (20)	In-plane CCH deformation
973.9 (0)	963.3 (0)	781.5 (0)	C_2H_2 torsion
882.6 (12)	880.8 (1)	661.1 (6)	In-plane CCH deformation
665.9 (66)	662.2 (87)	553.3 (28)	C_2H_2 tilt
588.4 (35)	572.8 (33)	505.8 (50)	symm Ge−C stretching
574.8 (60)	560.0 (55)	502.0 (53)	antisymm Ge−C stretching
		B3PW91	
3177.8 (9)	3164.9 (9)	2393.8 (1)	symm C−H stretching
3149.3 (9)	3140.0 (9)	2322.1 (3)	antisymm C−H stretching
1512.3 (6)	1457.1 (6)	1450.4 (5)	C−C stretching
1070.6 (64)	1053.6 (68)	911.1 (17)	In-plane CCH deformation
975.7 (0)	965.1 (0)	783.1 (0)	C_2H_2 torsion
882.4 (0.1)	8780.5 (0.3)	666.3 (9)	In-plane CCH deformation
670.8 (68)	667.2 (68)	562.4 (26)	C_2H_2 tilt
602.8 (37)	587.0 (35)	514.5 (54)	symm Ge−C stretching
591.4 (60)	576.4 (56)	509.7 (50)	antisymm Ge−C stretching

[a] Vibrational frequencies are given in reciprocal centimeters; intensities (in parentheses) are given in kilometers per mole.

TABLE 3: Calculated (B3LYP and B3PW91/6-311++G(d,p)) Vibrational Frequencies and Intensities of HGeCCH ($^1A'$)[a]

HGeCCH	HGe$^{13}C^{13}$CH	DGeCCD	mode
		B3LYP	
3451.9 (43)	3434.1 (45)	2671.9 (8)	C−H stretching
2060.9 (51)	1986.9 (46)	1931.8 (66)	C−C stretching
1890.8 (336)	1890.8 (336)	1351.0 (173)	Ge−H stretching
772.8 (31)	765.4 (31)	613.3 (14)	Out-of-plane CCH bending
756.3 (70)	753.6 (69)	572.3 (42)	HGeC bending
		B3PW91	
3456.2 (43)	3438.3 (44)	2676.3 (8)	C−H stretching
2066.4 (49)	1992.3 (44)	1936.4 (64)	C−C stretching
1914.2 (319)	1914.2 (319)	1367.7 (165)	Ge−H stretching
774.3 (31)	766.9 (31)	614.5 (14)	Out-of-plane CCH bending
753.8 (69)	751.1 (69)	571.3 (43)	HGeC bending

[a] Vibrational frequencies are given in reciprocal centimeters; intensities (in parentheses) are given in kilometers per mole.

stretching, CCH deformation, and C_2H_2 tilt modes are calculated at 1487.4, 1071.3, 640.8 cm^{-1} (Table 4) with the relative intensity ratio of 26/93/122. Experiments with different C_2H_2 concentration, laser energy, and deposition times have been performed, but the C−C stretching vibration with a weak intensity is not observed in the present experiment. The isotopic frequency ratio calculated for the CCH deformation and C_2H_2 tilt modes ($^{12}C_2H_2$/$^{13}C_2H_2$, 1.0122 and 1.0020) are also consistent with the experimental observations. These agreements between the experimental and the calculated vibrational frequencies, relative absorption intensities, and isotopic shifts confirm the identification of the Sn(C_2H_2) molecule from the matrix IR spectra.

HSnCCH. A new band at 1657.9 cm^{-1} with a site at 1652.8 cm^{-1} (Table 1 and Figure 5) appears on sample deposition, changes little on annealing to 25 and 30 K, sharply increases after broadband irradiation, and decreases on further annealing to 35 K. The band is assigned to the HSnCCH molecule on the basis of isotopic substitution and DFT calculations. The 1657.9 cm^{-1} band shows no carbon-13 shift but shifts to 1187.2 cm^{-1} with $^{12}C_2D_2$, exhibiting an isotopic frequency ratio of 1.3965 ($^{12}C_2H_2$/$^{12}C_2D_2$). The band position and the isotopic $^{12}C_2H_2$/$^{12}C_2D_2$ ratio are close to the values of the Sn−H stretching vibration of various previously characterized Sn hydrides in excess argon,[31] implying that the 1657.9 cm^{-1} band is due to a Sn−H stretching vibration. The mixed $^{12}C_2H_2$ + C_2D_2 isotopic spectra only provide the sum of pure isotopic bands, which indicates that only one Sn−H subunit is involved in this mode

TABLE 4: Calculated (B3LYP and B3PW91/6-311++G(d,p)-LANL2DZ) Vibrational Frequencies and Intensities of $Sn(C_2H_2)$ ($^1A_1$)[a]

$Sn(^{12}C_2H_2)$	$Sn(^{13}C_2H_2)$	$Sn(^{12}C_2D_2)$	mode
		B3LYP	
3136.9 (22)	3135.9 (24)	2356.3 (3)	symm C−H stretching
3107.9 (17)	3110.1 (17)	2289.5 (5)	antisymm C−H stretching
1487.4 (26)	1433.1 (24)	1431.8 (26)	C−C stretching
1071.3 (93)	1058.4 (97)	896.8 (32)	In-plane CCH deformation
949.7 (0)	942.4 (0)	759.7 (0)	C_2H_2 torsion
875.6 (18)	877.8 (1)	634.3 (3)	In-plane CCH deformation
640.8 (122)	639.5 (121)	485.5 (71)	C_2H_2 tilt
523.8 (70)	510.1 (64)	477.8 (28)	antisymm Sn−C stretching
493.3 (26)	478.5 (24)	460.9 (64)	symm Sn−C stretching
		B3PW91	
3150.4 (19)	3137.9 (20)	2368.1(2)	symm C−H stretching
3120.7(15)	3111.5 (15)	2299.2 (5)	antisymm C−H stretching
1499.1 (25)	1444.4(22)	1442.1 (24)	C−C stretching
1066.1 (94)	1050.5 (98)	894.3 (32)	In-plane CCH deformation
946.8 (0)	936.8 (0)	757.7 (0)	C_2H_2 torsion
873.8 (17)	872.7 (9)	633.6 (3)	In-plane CCH deformation
642.1 (100)	638.7 (123)	486.4 (73)	C_2H_2 tilt
532.7 (70)	518.3 (65)	482.6 (28)	antisymm Sn−C stretching
498.8 (26)	483.8 (24)	467.5 (64)	symm Sn−C stretching

[a] Vibrational frequencies are given in reciprocal centimeters; intensities (in parentheses) are given in kilometers per mole.

TABLE 5: Calculated (B3LYP and B3PW91/6-311++G(d,p)-LANL2DZ) Vibrational Frequencies and Intensities of HSnCCH ($^1A'$)[a]

HSnCCH	$HSn^{13}C^{13}CH$	DSnCCD	mode
		B3LYP	
3450.6 (37)	3432.7 (38)	2671.8 (8)	C−H stretching
2057.0 (42)	1983.2 (38)	1926.3 (56)	C−C stretching
1709.5 (447)	1709.5 (447)	1218.6 (229)	Sn−H stretching
739.7 (34)	733.1 (34)	582.6 (15)	Out-of-plane CCH bending
665.1 (85)	661.0 (97)	524.7 (15)	In-plane CCH bending
		B3PW91	
3453.9 (37)	3436.0 (38)	2675.5 (8)	C−H stretching
2060.6 (41)	1986.7 (37)	1928.9 (56)	C−C stretching
1706.3 (429	1706.3 (429)	1216.3 (219)	Sn−H stretching
742.7 (33)	736.1 (33)	584.8 (15)	Out-of-plane CCH bending
668.1 (72)	663.4 (80)	526.6 (16)	In-plane CCH bending

[a] Vibrational frequencies are given in reciprocal centimeters; intensities (in parentheses) are given in kilometers per mole.

(Figure 7). Therefore, 1657.9 cm^{-1} band is assigned to the Sn−H stretching vibration of the HSnCCH molecule.

The present calculations lend support for the assignment of HSnCCH. Our calculations predict that HSnCCH has an $^1A'$ ground state with C_s symmetry (Figure 10). The Sn−H stretching vibrational frequency is calculated at 1709.5 cm^{-1} (Table 5), which is in agreement with the experimental observations (1657.9 cm^{-1}). The calculated $^{12}C_2H_2/^{12}C_2D_2$ isotopic frequency ratio (1.4028) of Sn−H stretching mode is also consistent with the experimental observation (1.3965). The reason why the C−C stretching mode is not observed in the present experiment is due to its weak intensity as predicted by our DFT calculations. These agreements between the experimental and the calculated vibrational frequencies, relative absorption intensities, and isotopic shifts confirm the identification of the HSnCCH molecule from the matrix IR spectra.

Sn_2CCH_2. The absorption at 1445.4 cm^{-1} appears on annealing to 25 K, slightly increases upon further annealing to 30 K, and sharply decreases after broadband irradiation (Table 1 and Figure 4). The 1445.4 cm^{-1} band shifts to 1393.8 cm^{-1} with $^{13}C_2H_2$, exhibiting isotopic frequency ratios ($^{12}C_2H_2/^{13}C_2H_2$, 1.0370) characteristic of C−C stretching vibration. As shown in Figure 6, the mixed $^{12}C_2H_2 + {}^{13}C_2H_2$ isotopic spectra only provide the sum of pure isotopic bands, which indicates that only one C_2H_2 subunit is involved in this mode. In addition, the band is favored with larger laser energy, indicating more than one Sn atom are involved. The band is tentatively assigned to the Sn_2CCH_2 molecule.

TABLE 6: Calculated (B3LYP and B3PW91/6-311++G(d,p)-LANL2DZ) Vibrational Frequencies and Intensities of Sn_2CCH_2 ($^3B_1$)[a]

Sn_2CCH_2	$Sn_2{}^{13}C^{13}CH_2$	Sn_2CCD_2	mode
		B3LYP	
3111.5 (27)	3098.9 (27)	2323.2 (14)	C−H stretching
3050.2 (92)	3045.0 (92)	2222.1 (46)	C−H stretching
1525.2 (2)	1506.5 (2)	1413.4 (0)	C−C stretching
1371.6 (0.1)	1332.2 (0)	1066.3 (0)	Sn−C stretching
1050.6 (2)	1040.7 (2)	824.4 (3)	In-plane CCH deformation
908.6 (26)	899.0 (27)	728.1 (12)	Out-plane CCH deformation
		B3PW91	
3127.7 (22)	3114.9 (22)	2335.3 (11)	C−H stretching
3061.4 (87)	3055.9 (87)	2231.3 (44)	C−H stretching
1523.9 (2)	1501.5 (3)	1428.1 (0.2)	C−C stretching
1379.1 (0)	1343.0 (0)	1059.9 (0)	Sn−C stretching
1039.7 (2)	1030.1 (3)	814.3 (4)	In-plane CCH deformation
908.0 (26)	898.5 (27)	726.9 (11)	Out-plane CCH deformation

[a] Vibrational frequencies are given in reciprocal centimeters; intensities (in parentheses) are given in kilometers per mole.

TABLE 7: Calculated (B3LYP and B3PW91/6-311++G(d,p)-LANL2DZ) Vibrational Frequencies and Intensities of HPbCCH ($^1A'$)[a]

HPbCCH	$HPb^{13}C^{13}CH$	DPbCCD	mode
		B3LYP	
3448.2 (34)	3430.4 (34)	2668.8 (9)	C−H stretching
2049.3 (37)	1975.8 (33)	1919.5 (51)	C−C stretching
1604.8 (570)	1604.8 (570)	1142.0 (290)	Pb−H stretching
727.0 (40)	720.4 (40)	572.7 (18)	Out-of-plane CCH bending
661.6 (60)	656.2 (63)	520.9 (21)	In-plane CCH bending
		B3PW91	
3452.0 (33)	3445.9 (34)	2673.2 (8)	C−H stretching
2054.4 (36)	1981.5 (32)	1923.4 (50)	C−C stretching
1611.3 (550)	1617.6 (554)	1146.6 (280)	Pb−H stretching
729.4 (39)	725.1 (40)	574.4 (18)	Out-of-plane CCH bending
665.2 (59)	661.9 (62)	523.3 (21)	In-plane CCH bending

[a] Vibrational frequencies are given in reciprocal centimeters; intensities (in parentheses) are given in kilometers per mole.

Sn_2CCH_2 is predicted to have an $^3B_1$ ground state with C_{2v} symmetry, lying 1.6 and 32.9 kcal/mol lower in energy than the singlet and quintet ones, respectively, at the B3LYP level of theory (Figure 10). As shown in Figure 10, Sn_2 dimer elongates the C−C bond to 1.334 Å in Sn_2CCH_2 as compared with the 1.331 Å C−C bond in $Sn(C_2H_2)$. The C−C stretching frequency of Sn_2CCH_2 is calculated at 1525.2 cm^{-1} (Table 6), which is in agreement with our observed values 1445.4 cm^{-1}.

HPbCCH. A new band at 1541.3 cm^{-1} (Table 1 and Figure 8) appears on sample deposition, increases on annealing to 25 and 30 K, and disappears after broadband irradiation. The band is assigned to the HPbCCH molecule on the basis of isotopic substitution and DFT calculations. The 1541.3 cm^{-1} band shows no carbon-13 shift but shifts to 1105.6 cm^{-1} with $^{12}C_2D_2$, exhibiting isotopic frequency ratio of 1.3941 ($^{12}C_2H_2/^{12}C_2D_2$). The band position and the isotopic $^{12}C_2H_2/^{12}C_2D_2$ ratio are close to the values of the Pb−H stretching vibration of various previously characterized Pb hydrides in excess argon,[31] implying that the 1541.3 cm^{-1} band is due to a Pb−H stretching vibration. The mixed $^{12}C_2H_2 + {}^{12}C_2D_2$ isotopic spectra only provide the sum of pure isotopic bands, which indicates that only one Pb−H subunit is involved in this mode (Figure 9). Therefore, the 1541.3 cm^{-1} band is assigned to the Pb−H stretching vibration of the HPbCCH molecule.

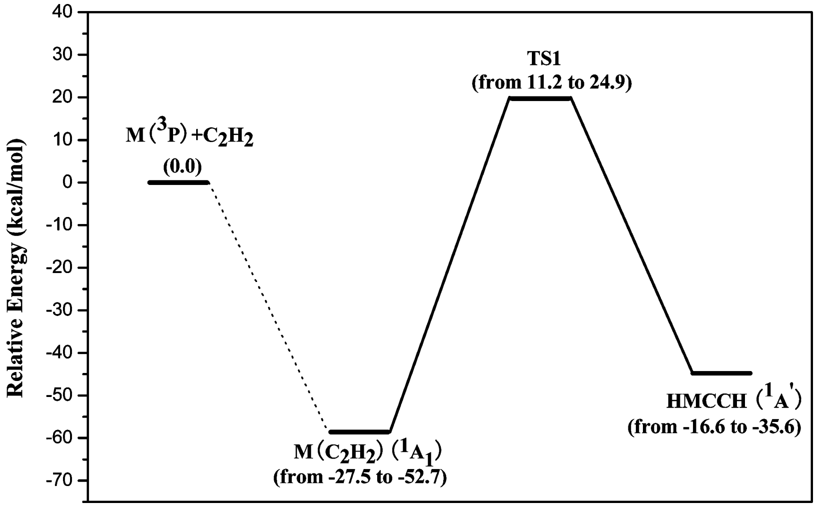

Figure 11. Potential energy surface for the reactions of group 14 metal atoms with acetylene calculated at the B3LYP/6-311++(d,p)-LANL2DZ level. Energies given are in kcal/mol and are relative to the separated ground-state reactants: $M(^3P) + C_2H_2(^1\Sigma_g^+)$.

The present calculations lend support for the assignment of HPbCCH. Our calculations predict that HPbCCH has an $^1A'$ ground state with C_s symmetry (Figure 10). The Pb−H stretching vibrational frequency is calculated at 1604.8 cm^{-1} (Table 7), which is in agreement with the experimental observation (1541.3 cm^{-1}). The calculated $^{12}C_2H_2/^{12}C_2D_2$ isotopic frequency ratio (1.4053) of Pb−H stretching mode is also consistent with the experimental observation (1.3941). The reason why the C−C stretching mode is not observed in the present experiment is its weak intensity as predicted by our DFT calculations. These agreements between the experimental and the calculated vibrational frequencies, relative absorption intensities, and isotopic shifts confirm the identification of the HPbCCH molecule from the matrix IR spectra.

Reaction Mechanism. Laser-ablated group 14 metal atoms react with C_2H_2 to form $Ge(C_2H_2)$, HGeCCH, $Sn(C_2H_2)$, HSnCCH, Sn_2CCH_2, and HPbCCH (Figures 1−9). According to reactions 1−7, the reactions are predicted to be exothermic by 52.7, 35.6, 35.9, 23.6, 22.3, and 16.6 kcal/mol, respectively. The $Ge(C_2H_2)$ and $Sn(C_2H_2)$ molecules disappear, while the HGeCCH and HSnCCH molecules increase after broadband irradiation, indicating that rearrangement reactions take place during broadband irradiation. For the reaction of laser-ablated Pb atoms with acetylene, only the HPbCCH product is observed. To have a better understanding of the rearrangement reactions, potential energy surfaces starting from M (M = Ge, Sn, and Pb) + C_2H_2 are calculated at the level of B3LYP, as shown in Figure 11. The ground-state ^3P group 14 metal atoms react with acetylene to form $^1A_1$ state $M(C_2H_2)$ molecule; the reaction is predicted to be all exothermic with minimal activation energy. A transition state has been located on the potential energy surfaces, which connect the equilibrium structure of $M(C_2H_2)$ with HMCCH. Therefore, plausible reaction mechanisms can be proposed as follows on the basis of the behavior of sample annealing and irradiation together with the observed species and calculated stable isomers. The group 14 metal atoms initially interact with the C−C triple bond of the C_2H_2 forming the $M(C_2H_2)$ complex. $M(C_2H_2)$ rearranges to HMCCH with barriers of 11.2, 21.1, and 24.9 kcal/mol for Ge, Sn, and Pb, respectively (Figure 11), which can be obtained by broadband irradiation or irradiation in the laser ablation plume during sample deposition. For the reaction of laser-ablated Pb atoms with acetylene, it is possible that irradiation in the laser ablation plume makes the adduct $Pb(C_2H_2)$ molecule isomerize to the HPbCCH molecule completely. Therefore, the $Pb(C_2H_2)$ molecule is not observed in the present experiments. It can be seen from Figure 1 that the IR absorption of Sn_2CCH_2 appears during sample deposition and visibly increases on annealing, suggesting that the Sn dimers can react with acetylene molecules to form the Sn_2CCH_2 molecule spontaneously according to reaction 5, which is predicted to be exothermic by 22.3 kcal/mol.

$$Ge(^3P) + C_2H_2(^1\sum_g^+) \rightarrow Ge(C_2H_2)(^1A_1) \qquad \Delta E = -52.7 \text{ kcal/mol} \quad (1)$$

$$Ge(^3P) + C_2H_2(^1\sum_g^+) \rightarrow HGeCCH(^1A') \qquad \Delta E = -35.6 \text{ kcal/mol} \quad (2)$$

$$Sn(^3P) + C_2H_2(^1\sum_g^+) \rightarrow Sn(C_2H_2)(^1A_1) \qquad \Delta E = -35.9 \text{ kcal/mol} \quad (3)$$

$$Sn(^3P) + C_2H_2(^1\sum_g^+) \rightarrow HSnCCH(^1A') \qquad \Delta E = -23.6 \text{ kcal/mol} \quad (4)$$

$$Sn_2(^3\sum_g^+) + C_2H_2(^1\sum_g^+) \rightarrow Sn_2CCH_2(^3B_1) \qquad \Delta E = -22.3 \text{ kcal/mol} \quad (5)$$

$$Pb(^3P) + C_2H_2(^1\sum_g^+) \rightarrow Pb(C_2H_2)(^1A_1) \qquad \Delta E = -27.5 \text{ kcal/mol} \quad (6)$$

$$Pb(^3P) + C_2H_2(^1\sum_g^+) \rightarrow HPbCCH(^1A') \qquad \Delta E = -16.6 \text{ kcal/mol} \quad (7)$$

Conclusions

Reactions of laser-ablated group 14 metal atoms with acetylene in excess argon have been studied using matrix-isolation infrared spectroscopy. On the basis of the isotopic shifts and splitting patterns, the $Ge(C_2H_2)$, HGeCCH, $Sn(C_2H_2)$, Sn_2CCH_2, HSnCCH, and HPbCCH molecules have been characterized. Density functional theory calculations have been performed, which lend strong support to the experimental assignments of the infrared spectra. In addition, a plausible reaction mechanism for the formation of the products has been proposed.

Acknowledgment. This work was supported by a Grant-in-Aid for Scientific Research (B) (Grant No. 17350012) from the Ministry of Education, Culture, Sports, Science and Technology (MEXT) of Japan. Y.-L.T. thanks JASSO and Kobe University for Honors Scholarship.

References and Notes

(1) Rashidi, M.; Puddephatt, R. J. *J. Am. Chem. Soc.* **1986**, *108*, 7111.

(2) Cremer, P. S.; Su, S. D.; Shen, Y. R.; Somorjai, G. A. *J. Phys. Chem. B* **1997**, *101*, 6474.

(3) Kose, R.; Brown, W. A.; King, D. A. *J. Am. Chem. Soc.* **1999**, *121*, 4845.

(4) Ozin, G. A.; McIntosh, D. F.; Power, W. J.; Messmer, R. P. *Inorg. Chem.* **1981**, *20*, 1782.

(5) Kasai, P. H. *J. Am. Chem. Soc.* **1982**, *104*, 1165.

(6) Kasai, P. H. *J. Am. Chem. Soc.* **1992**, *114*, 3299.

(7) Kline, E. S.; Kafafi, Z. H.; Hauge, R. H.; Margrave, J. L. *J. Am. Chem. Soc.* **1987**, *109*, 2402.

(8) (a) Burkholder, T. R.; Andrews, L. *Inorg. Chem.* **1993**, *32*, 2491. (b) Chertihin, G. V.; Andrews, L. *J. Am. Chem. Soc.* **1994**, *116*, 3513.

(9) (a) Manceron, L.; Andrews, L. *J. Am. Chem. Soc.* **1985**, *107*, 563. (b) Lee, Y. K.; Manceron, L.; Papai, I. *J. Phys. Chem. A* **1997**, *101*, 9650.

(10) Andrews, L.; Hassanzadeh, P.; Martin, J. M. L.; Taylor, P. R. *J. Phys. Chem.* **1993**, *97*, 5839.

(11) Thompson, C. A.; Andrews, L. *J. Am. Chem. Soc.* **1996**, *118*, 10242.

(12) Kline, E. S.; Kafafi, Z. H.; Hauge, R. H.; Margrave, J. L. *J. Am. Chem. Soc.* **1985**, *107*, 7559.

(13) Chenier, J. H. B.; Howard, J. A.; Mile, B.; Sutcliffe, R. *J. Am. Chem. Soc.* **1983**, *105*, 788.

(14) Huang, Z. G.; Zeng, A. H.; Dong, J.; Zhou, M. F. *J. Phys. Chem. A* **2003**, *107*, 2329.

(15) Wang, X. F.; Andrews, L. *J. Phys. Chem. A* **2004**, *108*, 4838.

(16) Wang, X. F.; Andrews, L. *J. Phys. Chem. A* **2003**, *107*, 337.

(17) Andrew, L.; Kushto, G. P.; Marsden, C. J. *Chem.—Eur. J.* **2006**, *12*, 8324.

(18) Cohen, D.; Basch, H. *J. Am. Chem. Soc.* **1983**, *105*, 6980.

(19) Sodupe, M.; Bauschlicher Jr, C. W. *J. Phys. Chem.* **1991**, *95*, 8640.

(20) Bauschlicher Jr, C. W.; Langhoff, S. R. *J. Phys. Chem.* **1991**, *95*, 2278.

(21) (a) Rosi, M.; Bauschlicher Jr, C. W. *Chem. Phys. Lett.* **1990**, *166*, 189. (b) Fournier, R. *Int. J. Quantum Chem.* **1994**, *52*, 973. (c) Bohme, M.; Wagener, T.; Frenking, G. *J. Organomet. Chem.* **1996**, *520*, 31.

(22) (a) Weidenbruch, M. *Angew. Chem., Int. Ed.* **2003**, *42*, 2222. (b) Miotto, R.; Ferraz, A. C. *Surf. Sci.* **2002**, *513*, 422.

(23) Zoellner, R. W.; Klabunde, K. J. *Inorg. Chem.* **1984**, *23*, 3241.

(24) (a) Zhou, M. F.; Andrews, L.; Bauschlicher, C. W. Jr. *Chem. Rev.* **2001**, *101*, 1931. (b) Himmel, H. J.; Downs, A. J.; Greene, T. M. *Chem. Rev.* **2002**, *102*, 4191, and references therein.

(25) (a) Burkholder, T. R.; Andrews, L. *J. Chem. Phys.* **1991**, *95*, 8697. (b) Zhou, M. F.; Tsumori, N.; Andrews, L.; Xu, Q. *J. Phys. Chem. A* **2003**, *107*, 2458. (c) Xu, Q.; Jiang, L.; Tsumori, N. *Angew. Chem., Int. Ed.* **2005**, *44*, 4338. (d) Jiang, L.; Xu, Q. *J. Am. Chem. Soc.* **2005**, *127*, 42. (e) Jiang, L.; Xu, Q. *J. Am. Chem. Soc.* **2005**, *127*, 8906.

(26) Frisch, M. J.; Trucks, G. W.; Schlegel, H. B.; Scuseria, G. E.; Robb, M. A.; Cheeseman, J. R.; Montgomery, J. A., Jr.; Vreven, T.; Kudin, K. N.; Burant, J. C.; Millam, J. M.; Iyengar, S. S.; Tomasi, J.; Barone, V.; Mennucci, B.; Cossi, M.; Scalmani, G.; Rega, N.; Petersson, G. A.; Nakatsuji, H.; Hada, M.; Ehara, M.; Toyota, K.; Fukuda, R.; Hasegawa, J.; Ishida, M.; Nakajima, T.; Honda, Y.; Kitao, O.; Nakai, H.; Klene, M.; Li, X.; Knox, J. E.; Hratchian, H. P.; Cross, J. B.; Adamo, C.; Jaramillo, J.; Gomperts, R.; Stratmann, R. E.; Yazyev, O.; Austin, A. J.; Cammi, R.; Pomelli, C.; Ochterski, J. W.; Ayala, P. Y.; Morokuma, K.; Voth, G. A.; Salvador, P.; Dannenberg, J. J.; Zakrzewski, V. G.; Dapprich, S.; Daniels, A. D.; Strain, M. C.; Farkas, O.; Malick, D. K.; Rabuck, A. D.; Raghavachari, K.; Foresman, J. B.; Ortiz, J. V.; Cui, Q.; Baboul, A. G.; Clifford, S.; Cioslowski, J.; Stefanov, B. B.; Liu, G.; Liashenko, A.; Piskorz, P.; Komaromi, I.; Martin, R. L.; Fox, D. J.; Keith, T.; Al-Laham, M. A.; Peng, C. Y.; Nanayakkara, A.; Challacombe, M.; Gill, P. M. W.; Johnson, B.; Chen, W.; Wong, M. W.; Gonzalez, C.; Pople, J. A. *Gaussian 03, revision B.04*; Gaussian, Inc.: Pittsburgh, PA, 2003.

(27) (a) Lee, C.; Yang, E.; Parr, R. G. *Phys. Rev. B* **1988**, *37*, 785. (b) Becke, A. D. *J. Chem. Phys.* **1993**, *98*, 5648.

(28) (a) Krishnan, R.; Binkley, J. S.; Seeger, R.; Pople, J. A. *J. Chem. Phys.* **1980**, *72*, 650. (b) Frisch, M. J.; Pople, J. A.; Binkley, J. S. *J. Chem. Phys.* **1984**, *80*, 3265.

(29) (a) Wachter, J. H. *J. Chem. Phys.* **1970**, *52*, 1033. (b) Hay, P. J. *J. Chem. Phys.* **1977**, *66*, 4377. (c) Hay, P. J.; Wadt, W. R. *J. Chem. Phys.* **1985**, *82*, 299.

(30) Cowieson, D. R.; Barnes, A. J.; Orville-Thomas, W. J. *J. Raman Spectrosc.* **1981**, *10*, 224.

(31) Wang, X. F.; Andrews, L. *J. Am. Chem. Soc.* **2003**, *125*, 6581.

JP902041F